

# The Clp1 Protein Is Required for Clamp Formation and Pathogenic Development of *Ustilago maydis*<sup>W</sup>

Mario Scherer, Kai Heimel, Verena Starke,<sup>1</sup> and Jörg Kämper<sup>2</sup>

Max-Planck-Institut für Terrestrische Mikrobiologie, Abteilung Organismische Interaktionen, D-35043 Marburg, Germany

In the phytopathogenic fungus *Ustilago maydis*, pathogenic development is controlled by a heterodimer of the two homeodomain proteins bE and bW, encoded by the *b*-mating-type locus. We have identified a *b*-dependently induced gene, *clampless1* (*clp1*), that is required for the proliferation of dikaryotic filaments in planta. We show that *U. maydis* hyphae develop structures functionally equivalent to clamp cells that participate in the distribution of nuclei during cell division. In *clp1* mutant strains, dikaryotic filaments penetrate the plant cuticle, but development is stalled before the first mitotic division, and the clamp-like structures are not formed. Although *clp1* is immediately activated upon *b*-induction on the transcriptional level, nuclear-localized Clp1 protein is first observed at the stage of plant penetration prior to the first cell division. Induced expression of *clp1* strongly interferes with *b*-dependent gene regulation and blocks *b*-dependent filament formation and *b*-dependent cell cycle arrest. We speculate that the Clp1 protein inhibits the activity of the bE/bW heterodimer to facilitate the cell cycle progression during hyphal growth.

## INTRODUCTION

The phytopathogenic Basidiomycete *Ustilago maydis* is the causal agent of the smut disease on maize (*Zea mays*). Similar to other smut fungi, *U. maydis* displays a dimorphic life style and grows in its haploid phase as a saprophytic yeast. Sexual development is initiated by fusion of two haploid sporidia. The resulting dikaryon is filamentous; however, at the initial stage only the apical cell of the hyphae is filled with cytoplasm, while the distal part consists of empty sections. Cell division is stalled until the dikaryon invades the plant via a specialized infection structure, the appressorium, and only after plant penetration is the true filament with multiple septated compartments formed. At the initial stage of infection, the hyphae traverse plant cells without an apparent host defense response. Plant cells remain alive until late in the infection process. At later stages, plant tumors are induced by the fungus, followed by massive proliferation of fungal hyphae, nuclear fusion, and the formation of diploid teliospores. Meiosis occurs upon spore germination, and a septated basidia is formed, from which haploid sporidia are released by successive budding events (for review, see Banuett, 1995; Kahmann and Kämper, 2004).

The crucial step for the infection process is the formation of the dikaryon. This process is controlled by the two mating type loci, termed *a* and *b* (Rowell and DeVay, 1954; Rowell, 1955; Holliday, 1961; Puhalla, 1970; Day et al., 1971). The biallelic *a*-locus encodes a pheromone/receptor system that is responsible for cell

recognition and cell fusion of the sporidia (Bölker et al., 1992; Spellig et al., 1994). After formation of the dikaryon, different alleles of the multiallelic *b*-mating type are the prerequisite to initiate the biotrophic stage (Holliday, 1961; Puhalla, 1968; Banuett and Herskowitz, 1989). The *b*-locus encodes two distinct homeodomain proteins, termed bE and bW, that form a heterodimer, but only if they derive from different alleles (Schulz et al., 1990; Gillissen et al., 1992; Kämper et al., 1995). The central role of the bE/bW heterodimer for pathogenic development was demonstrated by the construction of haploid strains with a hybrid *b*-locus expressing different alleles of *bE* and *bW* (Bölker et al., 1995). Such strains are solopathogenic (i.e., they are able to infect the host plant without a mating partner). The bE/bW heterodimer has been shown to bind elements (*b*-binding sites) in the promoter region of *b*-responsive genes (Romeis et al., 2000; Brachmann et al., 2001). It is conceivable that genes that are either directly regulated by the bE/bW heterodimer or that are indirectly regulated via a *b*-dependent regulatory cascade are involved in the establishment of the biotrophic phase. In several attempts, 21 *b*-regulated genes have been identified (Bohlmann et al., 1994; Schauwecker et al., 1995; Urban et al., 1996; Wösten et al., 1996; Brachmann et al., 2001, 2003), but with the exception of the mitogen-activated protein kinase *kpp6*, which is involved in appressorium formation (Brachmann et al., 2003), none of the genes tested so far have been linked to pathogenic development. A more detailed insight into the *b*-dependent processes was achieved using DNA arrays that allow monitoring of gene expression of ~90% of all *U. maydis* genes (M. Scherer and J. Kämper, unpublished data). Array analysis identified ~350 *b*-responsive genes that change their expression within a 12-h time course after formation of an active bE/bW heterodimer. Several of these *b*-regulated genes are involved in cell cycle control, mitosis, and DNA replication, consistent with the observed cell cycle arrest after *b*-induction that is released only upon plant infection (M. Scherer and J. Kämper, unpublished data).

In most dikaryotic Basidiomycetes, the proper distribution of the two genetically distinct nuclei during mitotic cell divisions is

<sup>1</sup> Current address: NASA Astrobiology Institute, Carnegie Institution, 1530 P Street NW, Washington, DC 20005.

<sup>2</sup> To whom correspondence should be addressed. E-mail kaemper@mpi-marburg.mpg.de; fax 49-6421-178-609.

The author responsible for distribution of materials integral to the findings presented in this article in accordance with the policy described in the Instructions for Authors (www.plantcell.org) is: Jörg Kämper (kaemper@mpi-marburg.mpg.de).

<sup>W</sup> Online version contains Web-only data.

www.plantcell.org/cgi/doi/10.1105/tpc.106.043521

ensured by the formation of clamps. Clamp cells develop at the most apical cell of the dikaryotic hyphae at the position where the future septum will be formed. The process starts with the formation of a backward-directed, hook-formed cell. Subsequently, the two nuclei in the lateral cell undergo a synchronous division. From the first dividing pair of nuclei, one nucleus migrates into the clamp primordium, while the other moves toward the apex of the hyphae. From the second dividing pair, one nucleus moves backward to the distal part of the hypha, while the other moves to the apical part. A septum formed at the base of the clamp cell entraps one nucleus within the clamp cell; a second septum is formed subapical to the clamp cell, creating an apical compartment with two nuclei and a distal compartment with one nucleus. Subsequently, the clamp cell fuses with the subapical compartment to reconstitute its dikaryotic status. In *Coprinopsis cinerea* and *Schizophyllum commune*, clamp cell initiation and nuclear division are controlled by the *A*-mating type, while clamp cell fusion is controlled by the *B*-mating type (Swiezynski and Day, 1960a, 1960b; Raper, 1966). The *A*-locus encodes two classes of homeodomain transcription factors that function in a similar way as the *bE/bW* proteins in *U. maydis* (reviewed in Casselton and Olesnick, 1998; Hiscock and Kües, 1999; reviewed in Casselton, 2002). The *B*-locus encodes pheromones and the corresponding receptors that are discussed to mediate the fusion of the clamp via an extracellular communication of the genetically diverse cells (Kües, 2000; Brown and Casselton, 2001; Kothe, 2001).

In *U. maydis*, clamp-like structures are present in the dikaryotic stage; however, it has not been observed that these structures are involved in the distribution of nuclei. In particular, the fact that a fusion of the clamp-like cells to the distal hyphal compartment has not been observed prompted the conclusion that these structures are not the functional homologues of clamps (Snetselaar and Mims, 1994; Banuett and Herskowitz, 1996).

Here, we show that the clamp-like structures are involved in the distribution of nuclei in the hyphae of *U. maydis*. We have identified a *b*-dependently expressed gene encoding a protein with similarities to the Clpless1 (Clp1) protein from *C. cinerea*. In this higher Basidiomycete, it is necessary and sufficient to induce clamp formation (Inada et al., 2001). In *U. maydis*, *clp1* is required for the formation of the clamp-like structures. Strains deleted for *clp1* are still able to penetrate the plant cuticle; however, the tip cells of the filaments are unable to undergo mitotic divisions, resulting in a block at the earliest stage of biotrophic development. Induced expression of *clp1* leads to a block of *b*-dependent filament formation and *b*-dependent cell cycle arrest. Concomitantly, *b*-dependent genes are downregulated. Most likely, the Clp1 protein is needed to stall the *b*-induced cell cycle control as a prerequisite for mitotic divisions.

## RESULTS

### *U. maydis clp1* Is *b*-Dependently Regulated

To identify genes that are regulated in dependency of the *bE/bW* heterodimer, we have performed microarray experiments with custom Affymetrix arrays that cover ~90% of the predicted 6902 *U. maydis* genes. In the haploid strains AB31 and AB33, the *bE1*

and *bW2* genes are under the control of the arabinose-inducible *crg1* promoter and the nitrate-inducible *nar1* promoter, respectively (Brachmann et al., 2001), allowing the initiation of *b*-dependent development in axenic culture. The change in expression upon *bE1/bW2* gene induction was monitored independently in both strains during a 12-h time course using strains AB32 and AB34, which harbor the incompatible combination *bE2* and *bW2*, as controls. We identified ~350 genes that were induced or repressed more than twofold at least at one time point during the 12-h time course in both AB31 and AB33. A detailed analysis of the DNA array experiments will be published elsewhere.

One of the genes identified as *b*-dependently regulated is *clp1* (annotated as um02438 at the MIPS *Ustilago maydis* DataBase; <http://mips.gsf.de/genre/proj/ustilago>). The array experiment suggests that expression of *clp1* is induced early after formation of the *bE1/bW2* heterodimer (data not shown). In strain AB31 (*a1 bE1<sup>crg1P</sup>/bW2<sup>crg1P</sup>*), *clp1* expression can be detected 2 h after *b*-induction by real-time RT PCR and peaks after 5 h. In the control strain AB32 (*a1 bE2<sup>crg1P</sup>/bW2<sup>crg1P</sup>*), *clp1* expression is not detectable (Figure 1A). The *b*-dependent expression profile of *clp1* in AB31 was confirmed by RNA gel blot analysis (Figure 1B). Similarly, when an active *bE/bW* heterodimer is formed upon mating of the two compatible haploid wild-type strains FB1 (*a1b1*) and FB2 (*a2b2*), a 1.6-kb *clp1* transcript is induced. When strains with compatible *a* but incompatible *b* alleles are mated, this transcript cannot be detected (Figure 1C). Surprisingly, RNA gel blot analysis revealed the presence of a second, smaller *clp1* transcript of ~0.6 kb in size. The small transcript was detected (1) in mating reactions of strains with compatible *a* loci, (2) in the diploid strain FBD12-3 (*a1a2b1b1*), and (3) upon stimulation of FB1 (*a1b1*) with the *a2* pheromone, indicating an *a*-dependent regulation (Figure 1C).

### *U. maydis Clp1* Is Similar to the Clp1 Protein from *C. cinerea*

Inspection of the *clp1* cDNA obtained by 5'- and 3'-rapid amplification of cDNA ends did not reveal the presence of introns. *clp1* has 5'- and 3'-untranslated regions of 88 and 94 bp, respectively, and the gene encodes a potential protein of 444 amino acids. Two sequence motifs with high similarity to the *b*-binding sites in the promoter regions of the directly *b*-regulated genes *lga2* (Romeis et al., 2000) and *frb52* (Brachmann et al., 2001) at positions -252 and -1054 suggest that *clp1* is a direct *b*-target gene (Figures 2A and 2B). The deduced protein sequence of *clp1* shows weak similarity to Clp1 of *C. cinerea* (23% identities and 41% positives in a window of 282 amino acids at the C terminus). Clp1 in *C. cinerea* was found to be essential for *A*-dependent clamp formation, and forced expression of Clp1 bypassed the requirement for an active *A*-pathway for clamp formation (Inada et al., 2001). The genome of *C. cinerea* contains one additional predicted gene with similarity to *clp1*. Likewise, the genome of the second sequenced Homobasidiomycete, *Phanerochaete chrysosporium*, contains two sequences with *clp1* similarity, while that of *Cryptococcus neoformans* (belonging to the Filobasidiales) contains only one. Comparison of the deduced proteins did not reveal any conserved regions shared among all Clp1-related proteins nor the presence of any known structural motifs (see Supplemental Figure 1 online). Outside the

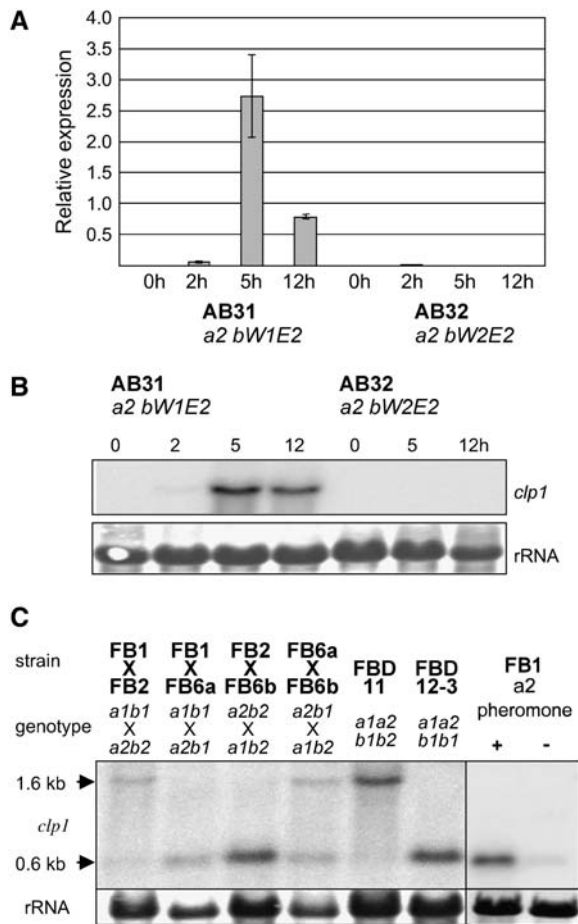


**Figure 1.** a- and b-Dependent Expression of *clp1*.

(A) and (B) Analysis of *clp1* expression after induction of compatible (strain AB31) and incompatible (strain AB32) combinations of *bE* and *bW*. Samples were taken before and 2, 5, and 12 h after induction with arabinose.

(A) Real-time quantitative RT-PCR analysis. *clp1* expression was measured relative to the constitutively expressed gene for peptidylprolyl isomerase (*ppi*; um03726). Shown are the mean values and standard deviation of four technical replicates.

(B) RNA gel blot analysis; 10  $\mu$ g of total RNA was loaded per lane. As a loading control, the filter was stained with methylene blue to visualize blotted rRNA.

(C) Wild-type strains FB1, FB2, FB6a, and FB6b and the diploid strains FBD11 and FBD12-3 were grown for 48 h on complete medium containing charcoal as indicated, prior to RNA isolation. FB1 was treated with pheromone a2 for 75 min. The probe used for hybridization covered 744 bp of the 5'-region of the *clp1* ORF. Note that only in combinations with an active *b1/b2* combination is the 1.6-kb *clp1* transcript visible; the smaller 0.6-kb transcript is formed in combinations with an active *a1/a2* combination.

Basidiomycete phylum, no sequences with similarities to Clp1 were found.

To elucidate whether the a-dependent transcript has the capacity to encode a protein, we aimed to isolate the corresponding cDNA from pheromone-treated FB1 cells; under this

condition, only the small transcript is detectable. Because all attempts using poly(dT) primers for cDNA synthesis failed, we used circular RT-PCR (cRT-PCR), a method that is suitable to generate cDNA from nonpolyadenylated RNAs (Couttet et al., 1997). We obtained a cDNA of 555 bp that covers 437 bp of the *clp1* open reading frame (ORF) and an additional 118 bp upstream region (Figure 2A). Sequence inspection revealed that the a-dependent transcript lacks a poly(A) tail; however, the 3'-end of the mRNA is predicted to form a stable secondary structure (Figure 2C). The ORF deduced from the short transcript lacks an in-frame stop codon and thus has no coding potential.

### *clp1* Is Required for Pathogenic Development

The *clp1* ORF was replaced by a hygromycin resistance cassette in *U. maydis* wild-type strains FB1 (*a1b1*) and FB2 (*a2b2*) and the haploid solopathogenic strain SG200 (*a1mfa2bE1bW2*). Deletion of *clp1* did not cause any obvious phenotype in haploid cells growing in axenic culture. The growth rate in minimal or complete media was not altered, and the mating reaction of the FB1 $\Delta$ *clp1* and FB2 $\Delta$ *clp1* (UVO161 and UVO162, respectively) strains was indistinguishable from that of the respective wild-type strains (data not shown). However, pathogenic development was strongly affected. Maize plants infected with a mixture of the strains FB1 $\Delta$ *clp1* and FB2 $\Delta$ *clp1* still showed chlorosis, but formation of tumors was not observed (Table 1). Similar results were obtained for the *clp1* deletion in the solopathogenic strain

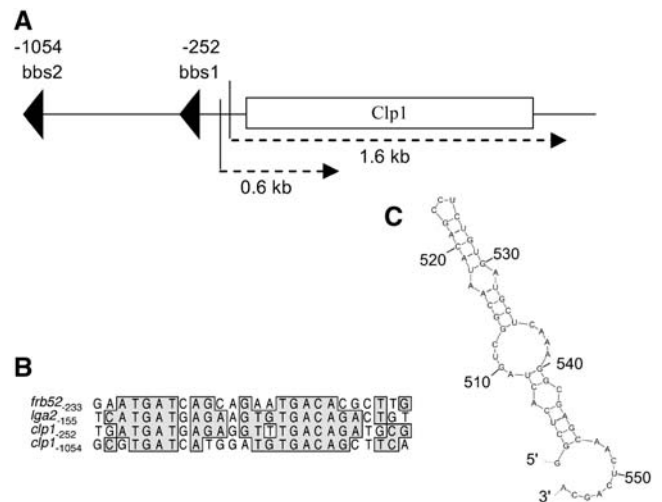


**Figure 2.** Structure of the *clp1* Gene.

(A) Schematic presentation of the *clp1* locus. Two potential *b*-binding sites and the two different transcripts (1.6 and 0.6 kb) are indicated.

(B) Alignment of the two potential *b*-binding sites within the *clp1* promoter to the binding sites within the *lga2* and *frb52* promoters (Romeis et al., 2000; Brachmann et al., 2001). Numbers indicate the position of the sequences with respect to the ATG start codon of the genes. Identical nucleotides are boxed.

(C) Potential secondary structure at the 3'-end of the small 0.6-kb transcript. The secondary structure was predicted using the mfold program (Zuker, 2003). The calculated initial  $\Delta$ G for the structure is  $-16.2$  kcal/mol.

**Table 1.** Pathogenicity of *clp1* Deletion Strains

Strains Inoculated	No. of Plants	Tumor Formation (%)
FB1 × FB2	61	96
FB1Δ <i>clp1</i> × FB2Δ <i>clp1</i>	62	0
SG200	18	94
SG200Δ <i>clp1</i>	38	0

Six-day-old maize plants were inoculated with the strains indicated, and tumor formation was scored 10 to 14 d after infection.

SG200, indicating (1) that the pathogenicity defect is not due to a defect in cell recognition or cell fusion and (2) that the requirement for *clp1* during pathogenic development is not connected to the dikaryotic stage per se. To determine at which stage the *clp1* mutants are blocked during pathogenic development, fungal cells in infected leaves were visualized by staining with Chlorazole Black E. As control for the infection experiments, we used the solopathogenic strain UMS71, a SG200 derivative expressing enhanced green fluorescent protein (eGFP) linked to a nuclear localization sequence (see below). Three days after inoculation, UMS71 had entered the plant via appressoria-like penetration structures, and massive proliferation of fungal material was observed in the leaf tissue. Typical clamp-like structures with Y-shaped septa (Snetselaar and Mims, 1994; Banuett and Herskowitz, 1996) were frequently found (Figure 3A). The *clp1* deletion strain UMS71Δ*clp1* (UMS67) showed no defect in appressoria formation and was able to invade the leaf tissue (Figure 3C1). However, no proliferation of fungal cells could be observed. Mostly, invading hyphae were short and restricted to single plant cells of the outer epidermal layer. Only in few cases did we observe that the hyphae surpassed more than one plant cell (Figure 3C2). Clamp-like structures were completely absent in the *clp1* mutant strain (Figure 3C2).

### Clamp-Like Structures in *U. maydis* Participate in Nuclear Distribution in Heterodikaryotic Hyphae

Although clamp-like structures formed by *U. maydis* during proliferative growth in planta have been described previously, a function with respect to nuclear distribution during cell divisions of the heterodikaryon has been excluded because the clamp cells do not fuse with the distal hyphal compartment (Snetselaar and Mims, 1994; Banuett and Herskowitz, 1996). To allow live imaging of nuclei in the dikaryotic hyphae of *U. maydis* during plant infection, we fused the ORF of eGFP arranged triple in tandem orientation (3xeGFP) to the nuclear localization signal (NLS) from VP16 that has been proven to be functional in *U. maydis* (Quadbeck-Seeger et al., 2000). NLS-3xeGFP was expressed under control of the *mig2-5* promoter, which is strongly induced in planta (Farfaring et al., 2005; Basse and Farfaring, 2006). When a mixture of strains FB1 and FB2, both expressing NLS-3xeGFP (UMS73 and UMS74, respectively), were coinjected into maize plants, nuclei showed strong fluorescence after the heterodikaryotic hyphae had penetrated the plant. At 48 h after inoculation, the clamp-like structures were observed at various stages of development. Initially, a branch-like structure

was formed; upon mitotic cell division, (1) either two nuclei were found within the branch, and the other two nuclei were positioned distal and proximal to the position of the branch (Figure 4A), or (2) only one nucleus was localized in the branch, one distal to the branch and two in the proximal part of the hypha (Figure 4B). Surprisingly, the nucleus located within the branch remained at this position in situations where the cell of the clamp-like structure was separated from the main hypha by a Y-shaped septum. By that, the nucleus appears to be trapped in the clamp-like structure (Figure 4B). In other Basidiomycetes, the subapical cell and the clamp fuse to release the trapped nucleus. Concomitantly with the observations of others, we did not observe a visible dissolution of the cell wall between the cell of the clamp-like structure and the subapical cell in *U. maydis*. Nevertheless, the nucleus moved out of the clamp-like structure into the subapical hyphal compartment. During this process, the nucleus often appeared as an elongated structure, of which parts still resided in the clamp-like structure, while the other part could be localized within the distal cell compartment; both parts of the nucleus were connected via thin projections (Figures 4C and 4D). Finally, the apical and subapical cell contained one pair of nuclei each (Figure 4E). Our data clearly demonstrate that clamp-like structures of *U. maydis* participate in nuclear distribution during division of heterodikaryotic hyphae. The solopathogenic strain UMS71 (SG200:NLS-3xeGFP) formed clamp-like structures as well (Figures 4F to 4H), although it proliferates in planta as a haploid monokaryon. During proliferation in planta, we observed that upon nuclear division one of the two daughter nuclei migrates into the clamp-like structure, while the second nucleus is positioned in the apical part of the hypha (Figure 4G). After formation of the Y-shaped septum, the nucleus migrates from the clamp-like structure to the distal cell, similar to the situation found in the dikaryon (Figure 4H).

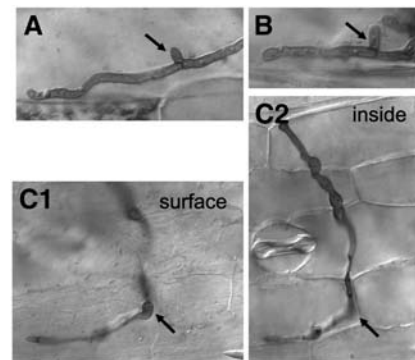


**Figure 3.** *clp1* Is Required for Proliferation in Planta during Pathogenic Development.

Infected leaves were stained with Chlorazole Black E 3 d after inoculation. Hyphae of the solopathogenic strains UMS71 (*a1mfa2bE1/bW2:NLS-3xeGFP*) (A) and CL13 (*a1bE1/bW2*) (B) form clamp-like structures in planta (arrows). Hyphae of strain UMS71Δ*clp1* can form appressoria (C1, arrow; focus on the leaf surface) and penetrate, but clamp-like structures are not observed. Fungal proliferation stops at latest when the hyphae have grown through two to three plant cells (C2; focus within the epidermal cell layer). The site of penetration is marked with an arrow.

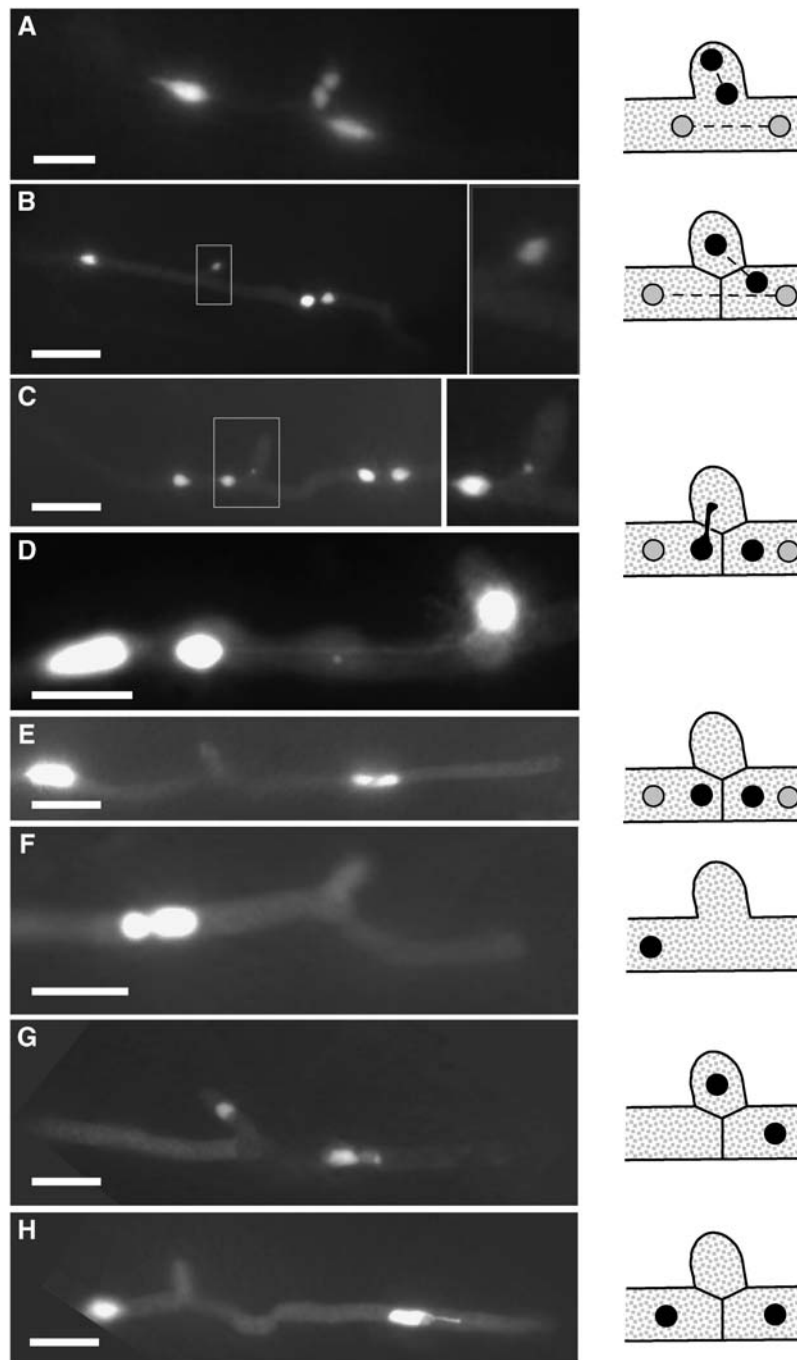


**Figure 4.** Clamp-Like Structures Participate in Nuclear Distribution.

**(A) to (E)** Dikaryotic hyphae of crosses of strains UMS73 (*a1b1*) and UMS74 (*a2b2*).

**(F) to (H)** Hyphae of the haploid solopathogenic strain UMS71 (*a1mfa2bE1/bW2*); all strains express a nuclear-localized NLS-3xeGFP; nuclei are visualized by fluorescence microscopy. Samples were taken 48 h after inoculation of maize plants.

Insets in **(B)** and **(C)** give an enlarged view of the clamp cell shown. The distribution of the nuclei with respect to the clamp cell is given in the illustrations at the right. For a detailed description, see text. Bars = 5  $\mu\text{m}$  in **(A)** and **(D)** and 10  $\mu\text{m}$  in all other panels.

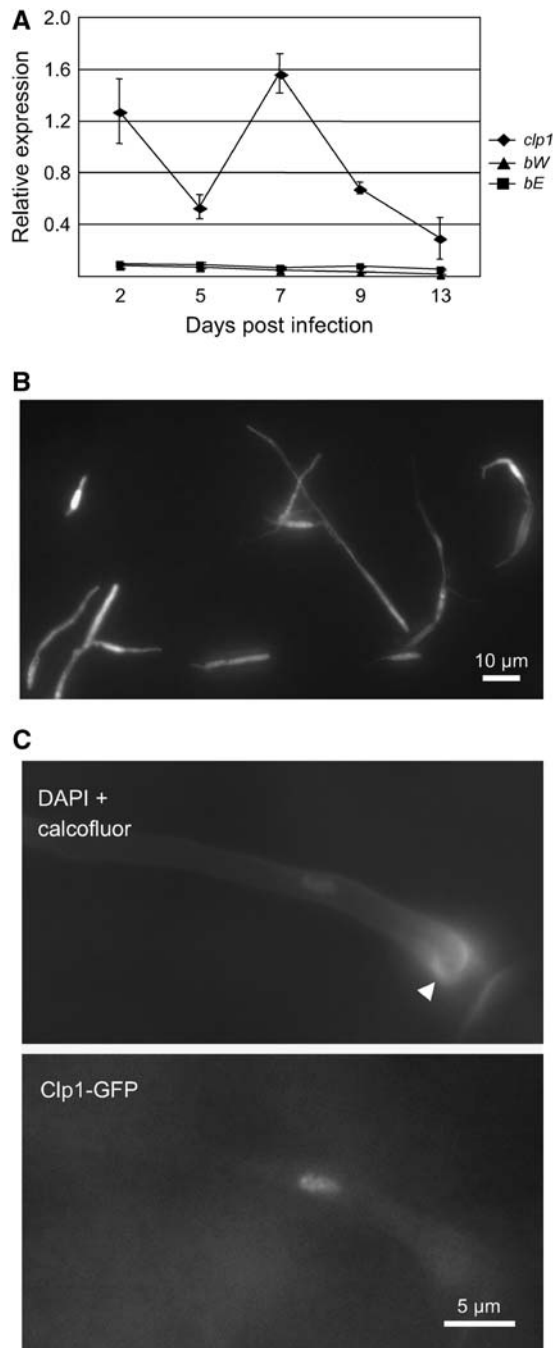


**Figure 5.** *clp1* Expression during Pathogenic Development.

**(A)** Real-time quantitative RT-PCR analysis of *clp1*, *bW*, and *bE* expression in planta. Samples from maize plants were taken 2, 5, 7, 9, and 13 d after infection with a mixture of compatible wild-type cells (FB1  $\times$  FB2). Expression was measured in relation to the constitutively expressed *ppi* gene. Shown are the mean values and standard deviation of four technical replicates.

**(B)** *clp1* gene expression during the early infection phase was monitored using a *clp1* promoter:eGFP reporter construct. The *clp1* ORF was replaced by eGFP in the solopathogenic strain SG200 by homologous recombination to create strain UMS76. eGFP expression of cells on a leaf

In the Basidiomycetes *C. cinerea* and *S. commune*, it is known that the formation of the clamp is dependent on the A-mating type locus, while fusion of the clamp cell with the distal cell compartment is dependent on the pheromone receptor system encoded by the B-locus (Kües, 2000; Brown and Casselton, 2001; Kothe, 2001). In *U. maydis*, we observed the formation of clamp-like structures in the solopathogenic strain CL13 (*a1bE1bW2*); since this strain is harboring only a single *a*-locus, we must assume that in contrast with other Basidiomycetes, the pheromone/receptor system is dispensable for the function of the clamp cells in *U. maydis* (Figure 3B).

### Clp1 Is Localized in the Nucleus and Is Posttranscriptionally Regulated

The expression of *clp1* during pathogenic development was analyzed by real-time RT-PCR using samples of tumor material collected 2, 5, 7, 9, and 13 d after infection with a mixture of the compatible wild-type strains FB1 (*a1b1*) and FB2 (*a2b2*). *clp1* expression was detectable at all time points, with a peak at 7 d after inoculation (Figure 5A). To address *clp1* expression on the plant surface prior to infection, the ORF was replaced with the ORF of the eGFP gene in the solopathogenic strain SG200. In the resulting strain, UMS76, we observed a bright GFP fluorescence in all hyphae on the leaf surface, indicating that *clp1* is expressed before hyphae penetrate the plant cuticle (Figure 5B).

To analyze the subcellular localization of the protein, the C terminus of Clp1 was fused to triple eGFP. The fusion construct was integrated into the *clp1* locus of the solopathogenic strain SG200, replacing the native *clp1* gene. The fusion protein was shown to be functional, since the resulting strain UMS48 infects maize plants with a rate similar to that of the respective unmodified strain SG200 (data not shown). When grown on the surface of maize leaves, the Clp1:3xeGFP fusion protein was localized in the nucleus of appressoria-like structures (Figure 5C); however, expression of the fusion protein was restricted to the stage of plant penetration. In no case did we detect the Clp1:eGFP signal in filaments prior to penetration (data not shown). Since *clp1* appears to be transcribed at a similar level in all cells, as judged from the eGFP expression levels of the *clp1*-promoter:*egfp* fusion, these observations suggest a posttranscriptional regulation of *clp1*.

### Overexpression of *clp1* Inhibits *b*-Dependent Filament Formation

In *C. cinerea*, expression of *clp1* is sufficient to initiate the formation of clamps in the absence of an active A-heterodimer,

surface 24 h after inoculation was monitored by fluorescence microscopy.

**(C)** Clp1:3xeGFP localizes to the nucleus of cells with appressoria (arrowhead). A functional *clp1*:3xeGFP fusion construct was expressed under control of the native *clp1* promoter in the strain SG200. Cells on the leaf surface were stained with 4',6-diamidino-2-phenylindole (DAPI) and calcofluor to visualize nuclei and appressoria (top panel). GFP fluorescence (bottom panel) shows the localization of the Clp1:3xeGFP fusion protein in the nucleus of a cell that has developed an appressorium.

suggesting a regulatory function downstream of *A* (Inada et al., 2001; Kamada, 2002). To test whether *U. maydis* *clp1* could have a similar function, we introduced an arabinose-inducible *clp1* allele into strain JB1 (*a1Δb*) that carries a deletion of the entire *b*-locus to create strain UVO151. After 2 h of growth in arabinose-containing medium, *clp1* expression was found to be drastically induced (Figure 6A). The induction of *clp1* in UVO151 did not change the morphology of the sporidia (data not shown). To address the question whether Clp1 exhibits its function as a transcriptional regulator, expression profiles of UVO151 and JB1 were compared 2 h after arabinose-induced expression of *clp1* by DNA microarray analysis. Data analysis revealed no significant changes in gene expression, with the exception of the 390-

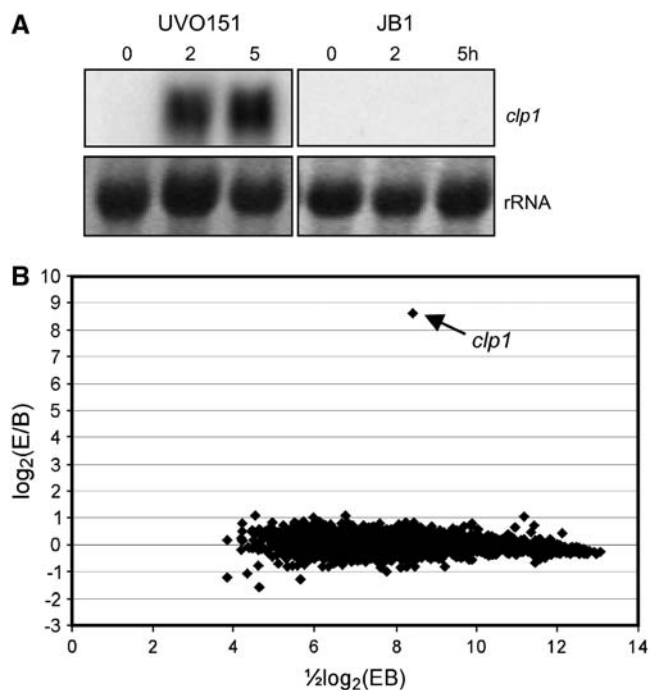


**Figure 6.** Clp1 Does Not Act as a Transcriptional Regulator by Itself.

(A) and (B) Strain UVO151 (*a1Δb crg1P:clp1*) is deleted for the entire *b*-locus and harbors an arabinose-inducible version of the *clp1* gene integrated into the *ip* locus as described (Brachmann et al., 2001). The expression of *clp1* was induced by 2 and 5 h of growth in arabinose-containing medium. As a control, strain JB1 (*a1Δb*) was grown under identical conditions.

(A) RNA gel blot analysis of *clp1* induction; 5  $\mu$ g of total RNA were loaded per lane. As a loading control, the filter was stained with methylene blue to visualize blotted rRNA. A  $^{32}$ P-labeled, 0.7-kb fragment of *clp1* was used as probe.

(B) MA plot (Yang et al., 2002) illustrating Affymetrix GeneChip results. Results represent two independent experiments. Expression profiles of UVO151 (experiment [E]) and JB1 (baseline [B]) were compared. Ratios of expression values were plotted versus signal intensities. Genes that were not consistently detected in either JB1 or UVO151 are not shown. Data analysis revealed no significant changes in gene expression, with the exception of the 390-fold-induced expression level of *clp1* (arrow). The entire data set can be viewed at <http://www.ncbi.nlm.nih.gov/projects/geo/> (accession number GSE4689).

fold-induced expression level of *clp1* (Figure 6B). Thus, it can be excluded that *U. maydis* Clp1 acts as a transcriptional regulator under these conditions.

Next, we were interested in the effect of Clp1 expression on *b*-dependent processes. The arabinose-inducible *clp1* allele was integrated into the *ip* locus of strain AB33, which carries the *bE1* and *bW2* genes under control of the nitrate-inducible *nar1* promoter. The resulting strain, UMS84, allows independent induction of Clp1 (by arabinose) and of an active bE/bW heterodimer (by nitrate). When cells were transferred to medium containing nitrate and glucose, leading to induction of *bE1/bW2* only, filament formation of UMS84 was comparable to that of AB33 (Figures 7A and 7B). Cell division of the filamentous cells was not observed, and nuclear staining with DAPI revealed that the filaments, comparable to AB33, contained a single nucleus, implying that the filaments are cell cycle arrested (Figures 7A and 7B). Simultaneous induction of *b* and *clp1* in UMS84 by nitrate/arabinose medium led to a drastic reduction of filamentation (Figure 7C) compared with the filaments formed by AB33 upon growth in nitrate/arabinose medium (Figure 7D). Less than 2% of the UMS84 cells exhibited filamentous growth after 20 h of induction compared with >90% filaments formed in strain AB33 under identical conditions. In medium containing glucose and Gln (i.e., under conditions where neither *b* nor *clp1* is induced), strains AB33, AB34 (harboring the inactive *bE2/bW2* combination), and UMS84 display a similar growth curve (Figure 7E, top panel). In medium containing glucose and nitrate (induction of *bE* and *bW*), in both AB33 and UMS84 cell divisions are stalled caused by the *b*-mediated cell cycle arrest, while growth of AB34 is unaffected (Figure 7E, middle panel). However, the simultaneous induction of *clp1* in arabinose/nitrate medium results in a growth rate of UMS84 that is comparable to that of AB34, indicating that the *b*-mediated cell cycle block must have been released (Figure 7E, bottom panel). Thus, both the change in cell morphology (sporidia instead of hyphae) and the cell cycle release indicate that Clp1 counteracts the function of the bE/bW heterodimer. Concomitantly, we observed a downregulation of *b*-dependent genes. The induction of *clp1*, driven by the *crg1* promoter in strain UMS84, leads to an expression level that is  $\sim 6$  times higher than the expression from the native *clp1* promoter after *b*-induction in strain AB33 (Figure 7F). The expression of the *bE* and *bW* genes, both under the control of the *nar1* promoter, is insignificantly altered after *clp1* induction (Figure 7F). However, under the same conditions, expression of the *b*-dependently expressed genes *lga2* (Romeis et al., 2000), *frb172* (Brachmann et al., 2001), *rep1* (Wösten et al., 1996), *kpp6* (Brachmann et al., 2003), *polX* (Brachmann et al., 2001), *dik6* (Bohlmann et al., 1994; G. Weinzierl and J. Kämper, unpublished data), *egl1* (Schauwecker et al., 1995), and *rbf1* (M. Scherer and J. Kämper, unpublished data) is strongly reduced in UMS84 compared with AB33 6 h after *b*-induction (Figure 7F).

## DISCUSSION

In *U. maydis*, the switch from saprophytic to biotrophic lifestyle and the morphological changes from budding to filamentous growth are closely interconnected. The dikaryotic hyphae formed upon fusion of two haploid sporidia initiate the biotrophic

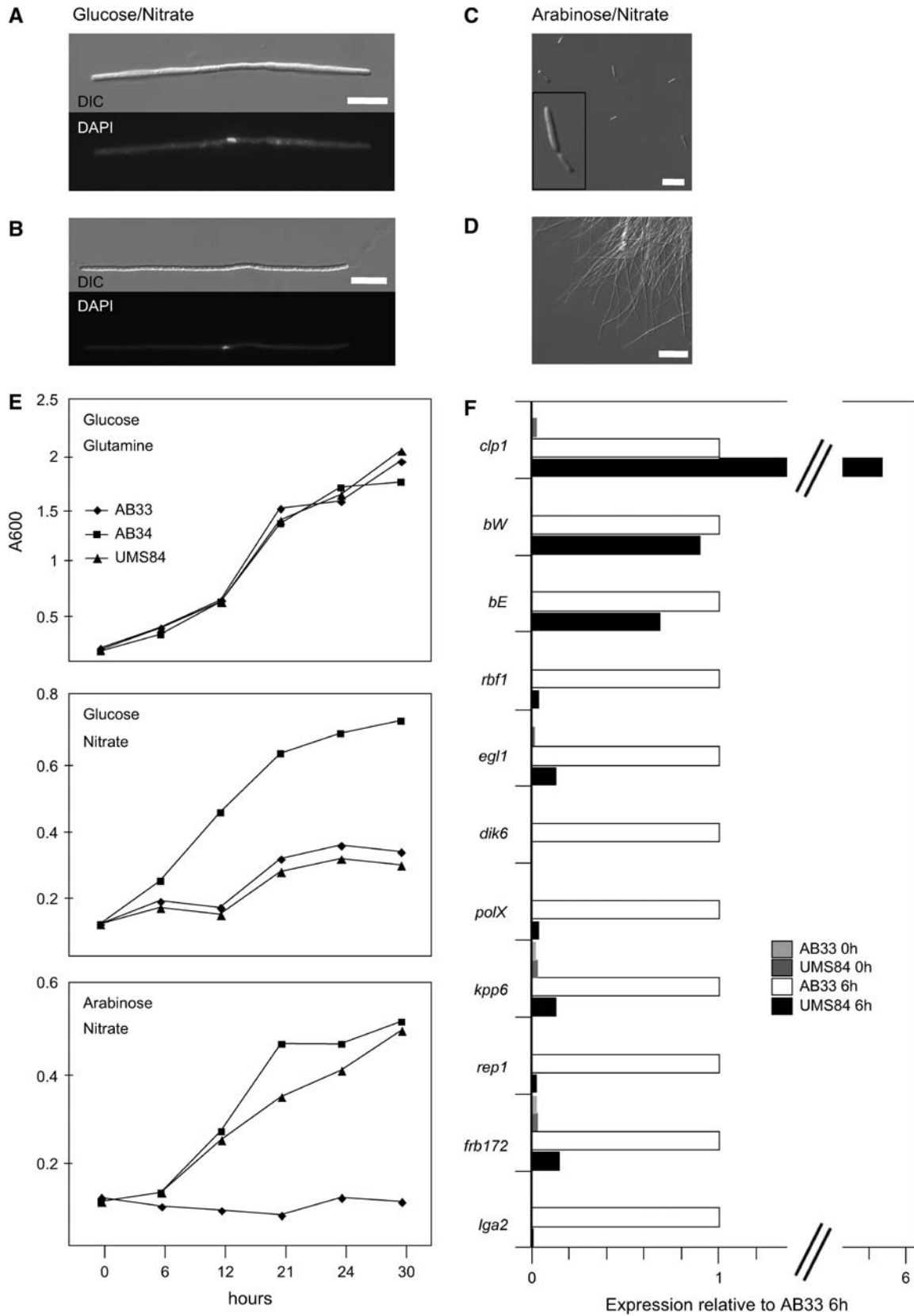


Figure 7. *clp1* Overexpression Inhibits *b*-Dependent Gene Regulation.

phase: without the host plant, cells do not divide any further. Only upon plant infection do the dikaryotic hyphae start to proliferate. In most Basidiomycetes, the proliferation of the dikaryon is accompanied by the formation of clamp cells that ensure the proper distribution of the genetically diverse nuclei. However, although widespread, clamps are not essential for the maintenance of a heterokaryotic mycelium; clampless dikaryons have been described in various cases (Swiezynski and Day, 1960a; Kemp, 1980; Salo et al., 1989), especially for various Uredinomyces (for recent examples, see Frieders and McLaughlin, 2001; Ikeda et al., 2003). Similarly, it was generally believed that in *U. maydis* clamps are not required for dikaryotic growth. Although dikaryotic filaments develop hyphal projections located at the septa of adjacent hyphal cells directly after penetration of the plant cuticle, these structures were generally considered to be branch primordia rather than true clamp connections, in particular because a fusion with the subapical hyphal cell was never observed (Sleumer, 1931; Snetselaar and Mims, 1994; Banuett and Herskowitz, 1996). Here, we provide evidence for a function of these clamp-like structures in the orderly distribution of nuclei using live imaging of the nuclei in dikaryotic hyphae. The formation of clamp-like structures of *U. maydis* shares several features with the formation of clamp connections in other Basidiomycetes: (1) The clamp-like projection is formed at the most apical cell of a dikaryotic hypha when the nuclei undergo coordinated division. (2) It is placed at the position of future septum formation. (3) One of the four resulting nuclei becomes located in the clamp-like structure and (4) is trapped there after septa have been formed. However, there are major differences with respect to the way the trapped nucleus is released to the subapical hyphal cell. In most filamentous Basidiomycetes, this is achieved by the fusion of the backward-growing clamp with a peg formed by the subapical cell (Badalyan et al., 2004). By contrast, we observed neither changes in the shape of clamp-like structures during mitotic cell division nor a visible dissolution of the cell wall in *U. maydis*. Despite the integral appearance of the cell wall, the

clamp-located nucleus migrates into the subapical hyphal cell, obviously through a narrow opening. One possibility is that the opening is the result of a locally restricted dissolution of the cell wall and by that resembling mechanistically a fusion event comparable to that of other Basidiomycetes. Another possibility is that the clamp cell is separated by formation of a septum that is similarly structured as the porated septae in between hyphal compartments. Since the pori (Bauer et al., 1997) facilitate nuclear migration in between the compartments (for example, see Giesy and Day, 1965), a fusion event would be expendable. Such an explanation would be in line with the finding that clamp formation in *U. maydis* is independent from the presence of an active pheromone pathway that, in higher Basidiomycetes, is required for cell fusion.

Clamp-like structures were also found in the solopathogenic strains SG200 and CL13, although their hyphae contain only single nuclei. Similar observations have been made for *A<sub>mut</sub>B<sub>mut</sub>* monokaryons of *C. cinerea* that, comparable to *U. maydis* SG200, harbor self-activating alleles of the *A*- and *B*-loci (Swamy et al., 1984; Kües, 2000). Obviously, in both *C. cinerea* and *U. maydis*, clamp formation is a program that is closely interconnected with the mitotic division program of hyphal cells.

Taken together, we find significant functional similarity between the formation of clamp-like structures in *U. maydis* and the formation of clamp connections in other Basidiomycetes; however, further ultrastructural studies are needed to provide evidence whether clamp formation in *U. maydis* differs mechanistically from that of higher Basidiomycetes.

### Regulation of Clamp Formation by Clp1

We have identified the *U. maydis clp1* gene to be essential for clamp formation and pathogenic development. *clp1* expression is *b*-dependent, and the early induction of *clp1* upon *b*-activation as well as the presence of two promoter regions with similarity to the known *b*-binding sites make it likely that the gene is directly

**Figure 7.** (continued)

**(A) to (D)** Strains AB33 (*a1 bE1<sup>nar1P</sup>/bW2<sup>nar1P</sup>*), AB34 (*a1 bE2<sup>nar1P</sup>/bW2<sup>nar1P</sup>*), and UMS84 (*a1 bE1<sup>nar1P</sup>/bW2<sup>nar1P</sup>clp1<sup>erg1</sup>*) were grown in minimal medium with Gln and glucose to an OD<sub>600</sub> of 0.1 prior to induction. Expression of the *b*-genes was induced by nitrate, and *clp1* expression was induced by arabinose. Induction of the active bE1/bW2 combination in strains UMS84 **(A)** and AB33 **(B)** leads to the formation of filaments with single nuclei (DAPI stain, bottom panel). Simultaneous induction of *clp1* in strain UMS84 suppresses filamentation; the cells display a yeast-like phenotype **(C)**. Strain AB33 is filamentous under identical conditions **(D)**. DIC, differential interference contrast. Bars = 10 μm in **(A)**, **(B)**, and **(D)** and 20 μm in **(C)**.

**(E)** Growth curves of strains AB33, AB34, and UMS84. Top panel: In medium containing glucose (*clp1*-off) and Gln (*b*-off), all strains display a similar growth curve. Middle panel: In medium containing nitrate (*b*-on) and glucose (*clp1*-off), strains AB33 and UMS84, both harboring the compatible bE1/bW2 combination, are drastically reduced in growth compared with strain AB34 harboring the incompatible bE2/bW2 combination. Bottom panel: In medium containing nitrate (*b*-on) and arabinose (*clp1*-on in strain UMS84), the growth rate of AB34 and UMS84 are comparable, despite the compatible bE1/bW2 combination in strain UMS84.

**(F)** Quantitative real-time PCR analysis of *b*-dependently expressed genes. Strains AB33 and UMS84 were shifted to arabinose/nitrate medium to induce the bE1/bW2 genes and additionally in UMS84 the *clp1* gene. RNA was extracted before the shift (0 h) and 6 h after induction. Differences in expression of the monitored genes were calculated relative to the expression in AB33 6 h after induction of *b* (defined as 100%). Values were normalized to the expression of the constitutively expressed *ppi* gene. Given are the mean values of two technical replicates that gave similar results. The expression of the following *b*-induced genes was monitored: *lga2*, a gene with unknown function involved in mitochondrial fragmentation (Romeis et al., 2000; Bortfeld et al., 2004); *frb172*, encoding a protein with similarities to K<sup>+</sup>/H<sup>+</sup> antiporters (Brachmann et al., 2001); *rep1*, encoding a hydrophobic surface protein (Wösten et al., 1996); *kpp6*, encoding a mitogen-activated protein kinase involved in appressoria formation (Brachmann et al., 2003); *polX*, encoding a protein with weak similarities to polymerase X (Brachmann et al., 2001); *dik6*, encoding a seven-transmembrane domain protein with unknown functions (Bohlmann et al., 1994; G. Weinzierl and J. Kämper, unpublished data); *egl1*, encoding a cellulase (Schauwecker et al., 1995); and *rbf1*, encoding a zinc finger transcription factor (M. Scherer and J. Kämper, unpublished data).

regulated by the bE/bW heterodimer. The *clp1* deletion does not affect the initial stages of *b*-mediated development; neither the formation of the dikaryotic filament nor the formation of appressoria is altered. The hyphae are capable of penetrating the plant cuticle, indicating that the *b*-dependent infection process per se is unaffected. In wild-type hyphae, the plant penetration marks the earliest time point for the first mitotic cell division, which is accompanied by the formation of clamp-like structures. In the *clp1* mutant strains, however, we never observed clamp formation or cell divisions, and as a consequence, hyphal development was blocked directly after plant penetration. One of the obvious functions of the *b*-locus is the control of the mitotic cell cycle. Nuclear division is stalled in dikaryotic hyphae until the fungus penetrates the plant (Snetselaar and Mims, 1992), and induced expression of the *bE1/bW2* genes in strains AB31 or AB33 is sufficient to induce a G2 cell cycle arrest (J. Pérez-Martín, unpublished data). However, *bE* and *bW* are expressed during the entire biotrophic growth phase, and recently we were able to show by means of a temperature-sensitive *bE* allele that *b*-function is required for pathogenic development subsequent to invasion (R. Wahl and J. Kämper, unpublished data). Thus, to release the cell cycle block and to allow proliferation, the *b*-dependent regulation has to be adapted after plant penetration. We favor that such an adaptation of *b*-function is mediated by the Clp1 protein. First, in *clp1* deletion strains, the *b*-mediated block is obviously not released. In addition, our data show that induced expression of *clp1* in a strain with an active bE1/bW2 heterodimer is sufficient to counteract *b*-dependent filamentation and to release the *b*-induced cell cycle block. How is this *clp1*-mediated regulation achieved? Because induction of *clp1* in cells lacking an active bE/bW heterodimer causes no significant alterations of the transcription profile, it is improbable that Clp1 exerts its function as a transcriptional regulator. Second, in strain UMS84, the expression of various *b*-dependent genes is drastically reduced upon *clp1* overexpression, although the *bE* and *bW* expression itself is only insignificantly reduced. Thus, we favor a regulation via Clp1 at the posttranscriptional level, possibly by inhibition of the transactivation activity of the *b*-heterodimer via protein-protein interaction. The inhibition of the yeast regulator Gal4p by Gal80p is a well-studied example for this mode of action (Lohr et al., 1995). Another level of complexity is added by the downregulation of the *rbf1* gene. *rbf1* is a directly *b*-regulated gene encoding a zinc finger transcription factor required for the expression of the majority of *b*-regulated genes (M. Scherer and J. Kämper, unpublished data). It is expected that by the inactivation of bE/bW function in combination with the downregulation of *rbf1* the expression of most *b*-dependent genes is altered upon *clp1* induction.

Similar to the situation in *U. maydis*, the *C. cinerea clp1* gene is considered to be a direct target of the homeodomain proteins encoded by the *A*-locus. Clp1 is thought to act as a repressor of Pcc1, a potential HMG box transcription factor. A loss-of-function mutation in *pcc1* produces clamp cells uncoupled from the presence of active *A*- and *B*-mating-type loci; Pcc1 is thus thought to act as a repressor of clamp cell formation. The current model suggests that in *C. cinerea*, clamp formation is initiated by the Clp1-mediated release of Pcc1 repression, consistent with the observation that forced *clp1* expression leads to an initiation

of clamp formation independent from the *A*-mating-type locus. As in *U. maydis*, the Clp1-mediated control of Pcc1 is proposed to appear at the posttranscriptional level, since the expression of *pcc1* is not decreased upon *clp1* induction (Murata et al., 1998; Inada et al., 2001; Kamada, 2002). Thus, although the Clp1 proteins from *U. maydis* and *C. cinerea* do not share known structural motifs and lack regions of highly similar amino acid sequence, they appear to have a conserved mechanism of altering the function of key regulators of development.

In *U. maydis*, the Clp1 protein itself appears to be the subject of posttranscriptional regulation. Although the gene is expressed during the entire biotrophic stage, the protein can be detected within the nucleus only when the appressorium is formed (i.e., at the earliest detectable time when the cell cycle block can be released). It is possible that Clp1 transport to the nucleus is regulated (and the protein present in the cytoplasm is not detectable due to the lower concentration); alternatively, the translation or the stability of Clp1 could be regulated. It is tempting to speculate that a cyclic transport of Clp1 to the nucleus could set the timing

**Table 2.** Strains of *U. maydis* Used in This Study

Strain	Relevant Genotype	Reference
AB31	<i>a2 P<sub>crq</sub>:bW2,bE1</i>	Brachmann et al. (2001)
AB32	<i>a2 P<sub>crq</sub>:bW2,bE2</i>	Brachmann et al. (2001)
AB33	<i>a2 P<sub>nar</sub>:bW2,bE1</i>	Brachmann et al. (2001)
AB34	<i>a2 P<sub>nar</sub>:bW2,bE2</i>	Brachmann et al. (2001)
FB1	<i>a1 b1</i>	Banuett and Herskowitz (1989)
FB2	<i>a2 b2</i>	Banuett and Herskowitz (1989)
FB6a	<i>a2 b1</i>	Banuett and Herskowitz (1989)
FB6b	<i>a1 b2</i>	Banuett and Herskowitz (1989)
FBD11	<i>a1a2 b1b2</i>	Banuett and Herskowitz (1989)
FBD12-3	<i>a1a2 b1b1</i>	Banuett and Herskowitz (1989)
SG200	<i>a1mfa2 bW2bE1</i>	Bölker et al. (1995)
CL13	<i>a1 bW2bE1</i>	Bölker et al. (1995)
JB1	<i>a1 Δb::hph</i>	This study
UMS48	<i>a1mfa2 bW2bE1</i> <i>clp1:3xeGFP</i>	This study
UMS67	<i>a1mfa2 bW2bE1 Δclp1 ip<sup>r</sup></i> <i>[P<sub>mig2-5</sub>:NLS-3xeGFP]ip<sup>s</sup></i>	This study
UMS71	<i>a1mfa2 bW2bE1 ip<sup>r</sup></i> <i>[P<sub>mig2-5</sub>:NLS-3xeGFP]ip<sup>s</sup></i>	This study
UMS73	<i>a1 b1 ip<sup>r</sup>[P<sub>mig2-5</sub>:NLS-3xeGFP]</i> <i>ip<sup>s</sup></i>	This study
UMS74	<i>a2 b2 ip<sup>r</sup>[P<sub>mig2-5</sub>:NLS-3xeGFP]</i> <i>ip<sup>s</sup></i>	This study
UMS76	<i>a1mfa2 bW2bE1 P<sub>clp1</sub>:eGFP</i>	This study
UMS84	<i>a2 P<sub>nar</sub>:bW2,bE1 ip<sup>r</sup>[P<sub>crq</sub>:clp1]</i> <i>ip<sup>s</sup></i>	This study
UVO151	<i>a1 Δb ip<sup>r</sup>[P<sub>crq</sub>:clp1]ip<sup>s</sup></i>	This study
UVO159	<i>a1mfa2 bW2bE1 Δclp1</i>	This study
UVO161	<i>a1 b1 Δclp1</i>	This study
UVO162	<i>a2 b2 Δclp1</i>	This study

for the nuclear divisions during the entire biotrophic growth phase. Unfortunately, due to the weak signal of the Clp1:3xeGFP fusion protein, we were not able to detect any Clp1:3xeGFP protein signals after plant penetration.

In addition, *clp1* transcription appears to be regulated via the *a*-mediated signaling cascade. *a*-mediated induction leads to a truncated transcript, lacking a poly(A) tail and devoid of any coding capacity. It is possible that the transcript is the result of a stalled RNA polymerase or that it is caused by a premature abortion of transcription, triggered by a potential stem-loop structure formed during transcription. Both the mechanism of how this short transcript is generated and its potential function have to await further studies for clarification. However, since the *a*-locus is not required for clamp formation, an essential function of the short transcript for this process can be excluded.

With our work, we have provided insights into the molecular processes associated with the onset of hyphal proliferation after plant penetration of *U. maydis*. The first step in the dimorphic switch of *U. maydis* cells is the initiation of polarized growth leading to filament formation; this can be achieved on artificial media and has been well studied (Steinberg et al., 1998, 2001; Weber et al., 2003, 2006; Fuchs et al., 2005; Schuchardt et al., 2005). For the true filamentous growth, however, a multitude of different processes have to be coordinated to achieve synchronized nuclear divisions, sorting of nuclei, and cell differentiation. With our work, we have paved the road for the detailed study of these processes that are expected to be closely interwoven with the potential of *U. maydis* to infect its host plant. It will be of great interest to elucidate the particular role of the *b*-mating-type locus, especially to dissect its function with respect to the establishment of the pathogenicity program (i.e., those processes that facilitate infection) and to cope with the host environment, and the morphological program required for hyphal proliferation. We anticipate that this work will be of relevance not only to *U. maydis* but also to other Basidiomycetes and will lead to a better understanding of dikaryotic hyphal growth.

## METHODS

### Strains and Growth Conditions

*Escherichia coli* strain TOP10 (Invitrogen) was used for cloning purposes. *Ustilago maydis* cells were grown at 28°C in YEPS (Tsukuda et al., 1988), potato dextrose medium (Difco), complete medium, or minimal medium (Holliday, 1974). Mating assays and plant infections were performed as described by Gillissen et al. (1992). *U. maydis* strains used in this study are listed in Table 2.

### DNA and RNA Procedures

Molecular methods followed described protocols (Sambrook et al., 1989). DNA isolation from *U. maydis* and transformation procedures were performed as described (Schulz et al., 1990). Homologous integration of constructs was verified by gel blot analyses. Total RNA was extracted using Trizol reagent (Invitrogen) according to the manufacturer's instructions. RNA samples to be used for microarray analyses or real-time RT-PCR were further column purified (RNeasy; Qiagen) and the quality checked using a Bioanalyzer with an RNA 6000 Nano LabChip kit (Agilent). RNA ladder 3191 (Promega) was used as a size marker for RNA gel blot analyses. Membranes were stained for 5 min in 200 mg/mL

of methylene blue in 300 mM sodium acetate to assess equal loading and transfer. Probes for radioactive labeling of gel blots were generated by random priming (New England Biolabs). Detection and quantification of radioactive signals were performed with a STORM 840 PhosphorImager and ImageQuant 5.2 software (Molecular Dynamics).

### Real-Time RT-PCR

First-strand cDNA synthesis was performed using the SuperScript III first-strand synthesis SuperMix assay (Invitrogen) according to the manufacturer's protocol. As a template for the reaction, 1 µg of total RNA was used. Samples were incubated at 50°C for 50 min. Real-time PCR was performed on a Bio-Rad iCycler system using the Platinum SYBR Green qPCR SuperMix-UDG (Invitrogen) according to the manufacturer's protocol. Cycling conditions were as follows: 95°C for 2 min, 45 cycles of 30 s at 60°C, and 30 s at 72°C. After each PCR, the specificity of the amplifications was verified, and the threshold cycle above background was calculated using Bio-Rad iCycler software. Forward (F) and reverse (R) primers used for detection were as follows (in 5'–3' orientation): for *clp1*, *clp1*-F 5'-GTCAGTTCGTTTGCCTAC-3' and *clp1*-R 5'-GCATCGTCTCGTGCAACTTC-3'; for *bW*, *bW*-F 5'-GATCTCACCCAGCCAATCAC-3' and *bW*-R 5'-GAGTTGATCGAGCCGAATG-3'; for *bE*, *bE*-F 5'-GCAACACCTTCCATTGAC-3' and *bE*-R 5'-ACTGCTCCGAATGACT-3'; for *ppi*, *ppi*-F 5'-ACGCCGATTCACCTCGTC-3' and *ppi*-R 5'-TCTTGGCAGTCTTGGGAAC-3'; for *rbf1*, *RT\_rbf1\_F* 5'-AGTACGAGCTACGACG-GATTC-3' and *RT\_rbf1\_R* 5'-GGGTAGGTGTTGGACACATTC-3'; for *egl1*, *um06332RT\_1* 5'-CATCGCCAGATCCGTCACACC-3' and *um06332RT\_2* 5'-AAGTGTGACAGCGCCAACACTG-3'; for *dik6*, *um04130RT\_1* 5'-TTGTTCCACCCATCCTTACAGC-3' and *um04130RT\_2* 5'-GGATCGAGC-GTCGAAACACAGC-3'; for *polX*, *um01262RT\_1* 5'-GGATCGAGCGTC-GAAACACAGC-3' and *um01262RT\_2* 5'-GGATCGAGCGTCGAAACACAGC-3'; for *kpp6*, *um02331RT\_1* 5'-CTCCATTCTGACCTCCGCAAC-3' and *um02331RT\_2* 5'-GACAACACCATAGCGCCCTTCG-3'; for *rep1*, *um03924RT\_1* 5'-CCACTCCTTCGCCAAGCCTAC-3' and *um03924RT\_2* 5'-ACCGTCCAGGATGCCAATGTTG-3'; for *frb172*, *um04771RT\_1* 5'-AACACTCTGGCGCTCGTTCAGG-3' and *um04771RT\_2* 5'-GACCACTGAA-TCGATCCGCTGC-3'; and for *lga2*, *lga2RT\_1* 5'-TCTATCACGGGCAA-GAGGCTG-3' and *lga2RT\_2* 5'-ACTTTGCCGGTGACGACGTGAT-3'.

### cRT-PCR

The procedure used was modified from Couttet et al. (1997). Total RNA (20 µg) was decapped with 2.5 units of tobacco acid phosphatase (Invitrogen) for 2 h at 37°C. Decapped RNA was purified (RNeasy) and on-column DNase digested (DNase set; Qiagen). RNA (1 µg) was circularized with 10 units of T4 RNA ligase (New England Biolabs) in the supplied buffer supplemented with 40 units of RNaseOUT ribonuclease inhibitor (Invitrogen) for 16 h at 16°C. After phenol/chloroform extraction, RNA was precipitated with ethanol. First-strand cDNA synthesis was performed using Superscript II RNaseH<sup>-</sup> reverse transcriptase (Invitrogen) with the *clp1* gene-specific primer 5'-CGGATGTTGACATTGACGGGTGCG-3' for 1 h at 50°C. For PCR amplification, the nested primers 5'-TTGACGG-GTGCGAGAGGACGG-3' and 5'-TGTCACATCCGCAACTCTGCTAACCG-3' were used. cRT-PCR products were cloned using the TOPO cloning kit (Invitrogen).

### DNA Microarray Analysis

For DNA array analysis, custom-designed Affymetrix chips were used. Probe sets were designed based on the map-based sequencing assembly; for each predicted gene, 33 perfect match and the respective mismatch probes were designed, covering a region of 800 bp at the 3'-ends. The *U. maydis* DNA arrays address >6200 genes. Probe sets for the individual genes are available at <http://mips.gsf.de/genre/proj/ustilago/>.

For DNA array analysis, strains were grown to an OD<sub>600</sub> of 0.5 at 28°C in liquid array medium: 6.25% (w/v) salt solution, 30 mM L-Gln, and 1% (w/v) glucose, pH 7.0 (filter-sterilized). For induction of the *crg1* promoter, cells were inoculated in liquid array medium containing 1% (w/v) arabinose instead of glucose as a carbon source. Target preparation and hybridization were performed according to the standard Affymetrix protocol using the Enzo BioArray RNA transcript labeling kit, except for a reaction temperature of 50°C for first-strand cDNA synthesis. Experiments were done in two biological replicates. Hybridization followed the Affymetrix protocol, and arrays were processed following the EukGE-WS2 protocol on a GeneChip Fluidics Station 400 and scanned on an Affymetrix GSC2500. Data analysis was performed using the Affymetrix Micro Array Suite 5.0 software and the dChip1.3 program (<http://biosun1.harvard.edu/complab/dchip/>).

#### Tagging of Nuclei with Triple eGFP

To create plasmid pMS76, oligonucleotides NLS\_anti (5'-CATGCCGAA-TTCGACCTTTCTCTCTTTTTGGAGG-3') and NLS\_sense (5'-CATGG-TCGAGCCTCCAAAAAGAAGAGAAAGGTCGA-3') were hybridized and ligated to an *NcoI*-*NotI* 3xeGFP Hyg<sup>R</sup> fragment of pUMA647 (K. Zarnack and M. Feldbrügge, unpublished data) and an 869-bp *XbaI*-*NcoI* *mig2-5* promoter fragment of pJF (Farfing et al., 2005) and integrated into pRU12 (Brachmann et al., 2001), cut with *XbaI*-*NotI*. Correct orientation of the NLS was verified by PCR. pMS76 was linearized with *SspI* for integration into the *ip* locus of FB1, FB2, SG200, and UVO159 (Brachmann et al., 2001).

#### Deletion of *clp1*

The deletion of *clp1* was performed by a PCR-based approach (Kämper, 2004). The entire *clp1* ORF was replaced by a hygromycin resistance cassette in the strains FB1, FB2, and SG200.

#### Replacement of *clp1* by eGFP

pMS71 contains the *eGFP* gene fused to a 1-kb promoter region of *clp1*. The promoter region was amplified by PCR using primers 5'-GGTGGCCGCGTTGGCCGACATTATCATGATTGGGAATGGG-3' and 5'-AGATCGCGCCTGGAGCGC-3', generating an *SfiI* site at the 5'-end of *clp1*. The terminator region of *clp1* was amplified using primers 5'-GTGGCCTGAGTGGCCTGAATCCAACCATCAACGCCTC-3' and 5'-TTACGGAGCTCAAAGACACGC-3', generating an *SfiI* site at the 3'-end of *clp1*. Both fragments were ligated to an *SfiI* eGFP Hyg<sup>R</sup> fragment of pUMA317 in a pCR2.1 (Invitrogen) backbone. The eGFP Hyg<sup>R</sup> fragment in pUMA317 is similar to that of pMF3H (Brachmann et al., 2004) but contains an altered *SfiI* site (5'-GGCCAACGCGGCC-3') 5' to the eGFP ORF that allows translational in-frame fusions (P. Becht, J. König, and M. Feldbrügge, unpublished data). The fusion product was excised with *EcoRI* and integrated into the respective site of pUC18. Subsequently, the hygromycin resistance cassette was replaced by a nourseothricin resistance cassette as a *NotI* fragment from pSL-nat. pSL-nat harbors a 1.4-kb *NotI* fragment with the bacterial nourseothricin resistance gene, driven by the *U. maydis* GAPDH promoter and terminated by the *Saccharomyces cerevisiae* *cyc* terminator from plasmid pBR322-Nat1 (Kojic and Holloman, 2000; G. Bakkeren, personal communication). pMS71 was linearized with *SspI* for *U. maydis* transformation.

#### Clp1:eGFP Fusion

The 3'-region of the *clp1* ORF was amplified by PCR using primers 5'-GGTGGCCGCGTTGGCCGCTCGAGTTTGGTGGATTG-3' and 5'-TCC-CAGGTCAGCCTTTGCC-3', creating an *SfiI* site at the 3'-end. The 3' UTR sequence was amplified using primers 5'-GTGGCCTGAGTGGCCT-

GAATCCAACCATCAACGC-3' and 5'-TTACGGAGCTCAAAGACACGC-3', creating an *SfiI* site at the 5'-end. Both fragments were ligated to an *SfiI* 3xeGFP Hyg<sup>R</sup> fragment of pUMA647 (K. Zarnack and M. Feldbrügge, unpublished data) in a pCR2.1 vector (Invitrogen) to create pMS74.

#### Induced Expression of *clp1*

The *clp1* ORF was amplified by PCR from genomic DNA with the primers 5'-CATATGTCACCCCGTACCAGC-3' and 5'-GCGGCCGCTCACTC-GAGTTTGGTGGATTG-3', creating an *NdeI* site at the start and an *NotI* site following the stop codon. PCR products were cloned using the TOPO cloning kit (Invitrogen). After sequence verification, the *clp1* ORF was cloned as an *NdeI*-*NotI* fragment into the respective sites of pRU12 (Brachmann et al., 2001). The resulting plasmid pRU-ATG1 was linearized with *SspI* and transformed into strain AB33 (Brachmann et al., 2001) to yield strain UMS84 (*a2 P<sub>nar</sub>-bW2, bE1 ip*[*P<sub>crg</sub>:clp1*]*ip*<sup>8</sup>) or into strain JB1 (*a1Δb*) to yield strain UVO151 (*a1Δb ip*[*P<sub>crg</sub>:clp1*]*ip*<sup>8</sup>). JB1 (*a1Δb*) is a derivative of FB1 (Banuett and Herskowitz, 1989) in which the *b2*-locus was substituted with a 2.9-kb *PvuII* fragment harboring the hygromycin resistance cassette from plasmid pCM54 (Tsukuda et al., 1988), removing the entire *bE2* ORF and the *bW2* ORF to amino acid 624.

#### Microscopy

Microscopy analysis was performed using a Zeiss Axioplan 2 microscope. Photomicrographs were obtained with an Axiocam HrM camera, and the images were processed with Axiovision (Zeiss) and Photoshop (Adobe). For staining of nuclei with DAPI, Vectashield H-1200 (Vector Laboratories) was used. Cell wall components were stained with 2 μg/mL of Calcofluor-white (Sigma-Aldrich) in PBS. Chlorazole Black E staining of fungal cells in planta was performed as described (Brachmann et al., 2003).

#### Accession Numbers

Sequence data from this article can be found in the GenBank/EMBL data libraries under accession numbers XP\_758585.1 (*U. maydis clp1*, hypothetical protein UM02438.1 of the *U. maydis* 521 genome sequence) and AB034196 (*C. cinerea clp1*). DNA array data for the *clp1* induction were submitted to the National Center for Biotechnology Information Gene Expression Omnibus (<http://www.ncbi.nlm.nih.gov/projects/geo/>) under accession number GSE4689.

#### Supplemental Data

The following material is available in the online version of this article.

**Supplemental Figure 1.** Alignment of Clp1 to Predicted Proteins from Basidiomycetes.

#### ACKNOWLEDGMENTS

We thank M. Feldbrügge for various plasmid constructs, U. Kües, K. Snetselaar, and U. Kämper for stimulating discussions, J. Pérez-Martín for supplying unpublished data, and V. Vincon for his excellent technical support. This work was supported by grants from the German Ministry of Science and Education for the *U. maydis* DNA array setup, from the Max-Planck-Society for *U. maydis* genome annotation, and from the International Research Training Group Transcriptional Control of Developmental Processes of the German Research Foundation.

Received April 20, 2006; revised June 10, 2006; accepted July 20, 2006; published August 18, 2006.

## REFERENCES

- Badalyan, S.M., Polak, E., Hermann, R., Aebi, M., and Kues, U.** (2004). Role of peg formation in clamp cell fusion of homobasidiomycete fungi. *J. Basic Microbiol.* **44**, 167–177.
- Banuett, F.** (1995). Genetics of *Ustilago maydis*, a fungal pathogen that induces tumors in maize. *Annu. Rev. Genet.* **29**, 179–208.
- Banuett, F., and Herskowitz, I.** (1989). Different *a* alleles of *Ustilago maydis* are necessary for maintenance of filamentous growth but not for meiosis. *Proc. Natl. Acad. Sci. USA* **86**, 5878–5882.
- Banuett, F., and Herskowitz, I.** (1996). Discrete developmental stages during teliospore formation in the corn smut fungus, *Ustilago maydis*. *Development* **122**, 2965–2976.
- Basse, C.W., and Farsing, J.W.** (2006). Promoters and their regulation in *Ustilago maydis* and other phytopathogenic fungi. *FEMS Microbiol. Lett.* **254**, 208–216.
- Bauer, R., Oberwinkler, F., and Vanky, K.** (1997). Ultrastructural markers and systematics in smut fungi and allied taxa. *Can. J. Bot.* **75**, 1273–1314.
- Bohlmann, R., Schauwecker, F., Basse, C., and Kahmann, R.** (1994). Genetic regulation of mating and dimorphism in *Ustilago maydis*. In *Advances in Molecular Genetics of Plant-Microbe Interactions*, M.J. Daniels, ed (Dordrecht, The Netherlands: Kluwer Academic Publishers), pp. 239–245.
- Bortfeld, M., Auffarth, K., Kahmann, R., and Basse, C.W.** (2004). The *Ustilago maydis* *a2* mating-type locus genes *lga2* and *rga2* compromise pathogenicity in the absence of the mitochondrial *p32* family protein *Mrb1*. *Plant Cell* **16**, 2233–2248.
- Brachmann, A., König, J., Julius, C., and Feldbrugge, M.** (2004). A reverse genetic approach for generating gene replacement mutants in *Ustilago maydis*. *Mol. Genet. Genomics* **272**, 216–226.
- Brachmann, A., Schirawski, J., Müller, P., and Kahmann, R.** (2003). An unusual MAP kinase is required for efficient penetration of the plant surface by *Ustilago maydis*. *EMBO J.* **22**, 2199–2210.
- Brachmann, A., Weinzierl, G., Kämper, J., and Kahmann, R.** (2001). Identification of genes in the *bW/bE* regulatory cascade in *Ustilago maydis*. *Mol. Microbiol.* **42**, 1047–1063.
- Brown, A.J., and Casselton, L.A.** (2001). Mating in mushrooms: Increasing the chances but prolonging the affair. *Trends Genet.* **17**, 393–400.
- Bölker, M., Böhnert, H.U., Braun, K.H., Görl, J., and Kahmann, R.** (1995). Tagging pathogenicity genes in *Ustilago maydis* by restriction enzyme-mediated integration (REMI). *Mol. Gen. Genet.* **248**, 547–552.
- Bölker, M., Urban, M., and Kahmann, R.** (1992). The *a* mating type locus of *U. maydis* specifies cell signaling components. *Cell* **68**, 441–450.
- Casselton, L.A.** (2002). Mate recognition in fungi. *Heredity* **88**, 142–147.
- Casselton, L.A., and Olesnicky, N.S.** (1998). Molecular genetics of mating recognition in basidiomycete fungi. *Microbiol. Mol. Biol. Rev.* **62**, 55–70.
- Couttet, P., Fromont-Racine, M., Steel, D., Pictet, R., and Grange, T.** (1997). Messenger RNA deadenylation precedes decapping in mammalian cells. *Proc. Natl. Acad. Sci. USA* **94**, 5628–5633.
- Day, P.R., Anagnostakis, S.L., and Puhalla, J.E.** (1971). Pathogenicity resulting from mutation at the *b* locus of *Ustilago maydis*. *Proc. Natl. Acad. Sci. USA* **68**, 533–535.
- Farsing, J.W., Auffarth, K., and Basse, C.W.** (2005). Identification of cis-active elements in *Ustilago maydis* *mig2* promoters conferring high-level activity during pathogenic growth in maize. *Mol. Plant Microbe Interact.* **18**, 75–87.
- Frieders, E.M., and McLaughlin, D.J.** (2001). The heterobasidiomycete moss parasites *Jola* and *Eocronartium* in culture: Cytology, ultrastructure and anamorph. *Mycol. Res.* **105**, 734–744.
- Fuchs, U., Manns, I., and Steinberg, G.** (2005). Microtubules are dispensable for the initial pathogenic development but required for long-distance hyphal growth in the corn smut fungus *Ustilago maydis*. *Mol. Biol. Cell* **16**, 2746–2758.
- Giesy, R.M., and Day, P.R.** (1965). The septal pores of *Coprinus lagopus* in relation to nuclear migration. *Am. J. Bot.* **52**, 287–293.
- Gillissen, B., Bergemann, J., Sandmann, C., Schröer, B., Bölker, M., and Kahmann, R.** (1992). A two-component regulatory system for self/non-self recognition in *Ustilago maydis*. *Cell* **68**, 647–657.
- Hiscock, S.J., and Kües, U.** (1999). Cellular and molecular mechanisms of sexual incompatibility in plants and fungi. *Int. Rev. Cytol.* **193**, 165–295.
- Holliday, R.** (1961). The genetics of *Ustilago maydis*. *Genet. Res. Camb.* **2**, 204–230.
- Holliday, R.** (1974). *Ustilago maydis*. In *Handbook of Genetics*, R.C. King, ed (New York: Plenum Press), pp. 575–595.
- Ikeda, K.-I., Nakamura, H., and Matsumoto, N.** (2003). Mycelial incompatibility operative in pairings between single basidiospore isolates of *Helicobasidium mompa*. *Mycol. Res.* **107**, 847–853.
- Inada, K., Morimoto, Y., Arima, T., Murata, Y., and Kamada, T.** (2001). The *clp1* gene of the mushroom *Coprinus cinereus* is essential for *A*-regulated sexual development. *Genetics* **157**, 133–140.
- Kahmann, R., and Kämper, J.** (2004). *Ustilago maydis*: How its biology relates to pathogenic development. *New Phytol.* **164**, 31–42.
- Kamada, T.** (2002). Molecular genetics of sexual development in the mushroom *Coprinus cinereus*. *Bioessays* **24**, 449–459.
- Kämper, J.** (2004). A PCR-based system for highly efficient generation of gene replacement mutants in *Ustilago maydis*. *Mol. Genet. Genomics* **271**, 103–110.
- Kämper, J., Reichmann, M., Romeis, T., Bölker, M., and Kahmann, R.** (1995). Multiallelic recognition: Nonself-dependent dimerization of the *bE* and *bW* homeodomain proteins in *Ustilago maydis*. *Cell* **81**, 73–83.
- Kemp, R.F.O.** (1980). A heterothallic species of *Coprinus* related to *C. serquillinus* with clamp connections on homokaryotic and dikaryotic mycelia. *Trans. Br. Mycol. Soc.* **74**, 411–418.
- Kojic, M., and Holloman, W.K.** (2000). Shuttle vectors for genetic manipulations in *Ustilago maydis*. *Can. J. Microbiol.* **46**, 333–338.
- Kothe, E.** (2001). Mating-type genes for basidiomycete strain improvement in mushroom farming. *Appl. Microbiol. Biotechnol.* **56**, 602–612.
- Kües, U.** (2000). Life history and developmental processes in the basidiomycete *Coprinus cinereus*. *Microbiol. Mol. Biol. Rev.* **64**, 316–353.
- Lohr, D., Venkov, P., and Zlatanova, J.** (1995). Transcriptional regulation in the yeast *GAL* gene family: A complex genetic network. *FASEB J.* **9**, 777–787.
- Murata, Y., Fujii, M., Zolan, M.E., and Kamada, T.** (1998). Molecular analysis of *pcc1*, a gene that leads to *A*-regulated sexual morphogenesis in *Coprinus cinereus*. *Genetics* **149**, 1753–1761.
- Puhalla, J.E.** (1968). Compatibility reactions on solid medium and interstrain inhibition in *Ustilago maydis*. *Genetics* **60**, 461–474.
- Puhalla, J.E.** (1970). Genetic studies on the *b* incompatibility locus of *Ustilago maydis*. *Genet. Res. Camb.* **16**, 229–232.
- Quadbeck-Seeger, C., Wanner, G., Huber, S., Kahmann, R., and Kämper, J.** (2000). A protein with similarity to the human retinoblastoma binding protein 2 acts specifically as a repressor for genes regulated by the *b* mating type locus in *Ustilago maydis*. *Mol. Microbiol.* **38**, 154–166.
- Raper, J.R.** (1966). *Genetics of Sexuality in Higher Fungi*. (New York: The Ronald Press).
- Romeis, T., Brachmann, A., Kahmann, R., and Kämper, J.** (2000). Identification of a target gene for the *bE/bW* homeodomain protein complex in *Ustilago maydis*. *Mol. Microbiol.* **37**, 54–66.

- Rowell, J.B.** (1955). Functional role of compatibility factors and an *in vitro* test for sexual incompatibility with haploid lines of *Ustilago zeae*. *Phytopathology* **45**, 370–374.
- Rowell, J.B., and DeVay, J.E.** (1954). Genetics of *Ustilago zeae* in relation to basic problems of its pathogenicity. *Phytopathology* **44**, 356–362.
- Salo, V., Niini, S.S., Virtanen, I., and Raudaskoski, M.** (1989). Comparative immunocytochemistry of the cytoskeleton in filamentous fungi with dikaryotic and multinucleate hyphae. *J. Cell Sci.* **94**, 11–24.
- Sambrook, J., Frisch, E.F., and Maniatis, T.** (1989). *Molecular Cloning: A Laboratory Manual*. (Cold Spring Harbor, NY: Cold Spring Harbor Laboratory Press).
- Schauwecker, F., Wanner, G., and Kahmann, R.** (1995). Filament-specific expression of a cellulase gene in the dimorphic fungus *Ustilago maydis*. *Biol. Chem. Hoppe Seyler* **376**, 617–625.
- Schuchardt, I., Assmann, D., Thines, E., Schuberth, C., and Steinberg, G.** (2005). Myosin-V, Kinesin-1, and Kinesin-3 cooperate in hyphal growth of the fungus *Ustilago maydis*. *Mol. Biol. Cell* **16**, 5191–5201.
- Schulz, B., Banuett, F., Dahl, M., Schlesinger, R., Schäfer, W., Martin, T., Herskowitz, I., and Kahmann, R.** (1990). The *b* alleles of *U. maydis*, whose combinations program pathogenic development, code for polypeptides containing a homeodomain-related motif. *Cell* **60**, 295–306.
- Sleumer, O.** (1931). Über sexualität und zytologie von *Ustilago zeae* (Beckm.) Unger. *Zeitschr. Bot.* **25**, 209–262
- Snetselaar, K.M., and Mims, C.W.** (1992). Sporidial fusion and infection of maize seedlings by the smut fungus *Ustilago maydis*. *Mycologia* **84**, 193–203.
- Snetselaar, K.M., and Mims, C.W.** (1994). Light and electron microscopy of *Ustilago maydis* hyphae in maize. *Mycol. Res.* **98**, 347–355.
- Spellig, T., Bölker, M., Lottspeich, F., Frank, R.W., and Kahmann, R.** (1994). Pheromones trigger filamentous growth in *Ustilago maydis*. *EMBO J.* **13**, 1620–1627.
- Steinberg, G., Schliwa, M., Lehmler, C., Bolker, M., Kahmann, R., and McIntosh, J.R.** (1998). Kinesin from the plant pathogenic fungus *Ustilago maydis* is involved in vacuole formation and cytoplasmic migration. *J. Cell Sci.* **111**, 2235–2246.
- Steinberg, G., Wedlich-Soldner, R., Brill, M., and Schulz, I.** (2001). Microtubules in the fungal pathogen *Ustilago maydis* are highly dynamic and determine cell polarity. *J. Cell Sci.* **114**, 609–622.
- Swamy, S., Uno, I., and Ishikawa, T.** (1984). Morphogenic effects of mutations in the A and B incompatibility factors of *Coprinus cinereus*. *J. Gen. Microbiol.* **130**, 3219–3224.
- Swiezynski, K.M., and Day, P.R.** (1960a). Heterokaryon formation in *Coprinus lagopus*. *Genet. Res.* **1**, 114–128.
- Swiezynski, K.M., and Day, P.R.** (1960b). Migration of nuclei in *Coprinus lagopus*. *Genet. Res.* **1**, 129–139.
- Tsukuda, T., Carleton, S., Fotheringham, S., and Holloman, W.K.** (1988). Isolation and characterization of an autonomously replicating sequence from *Ustilago maydis*. *Mol. Cell. Biol.* **8**, 3703–3709.
- Urban, M., Kahmann, R., and Bölker, M.** (1996). Identification of the pheromone response element in *Ustilago maydis*. *Mol. Gen. Genet.* **251**, 31–37.
- Weber, I., Assmann, D., Thines, E., and Steinberg, G.** (2006). Polar localizing class V myosin chitin synthases are essential during early plant infection in the plant pathogenic fungus *Ustilago maydis*. *Plant Cell* **18**, 225–242.
- Weber, I., Gruber, C., and Steinberg, G.** (2003). A class-V myosin required for mating, hyphal growth, and pathogenicity in the dimorphic plant pathogen *Ustilago maydis*. *Plant Cell* **15**, 2826–2842.
- Wösten, H.A., Bohlmann, R., Eckerskorn, C., Lottspeich, F., Bölker, M., and Kahmann, R.** (1996). A novel class of small amphipathic peptides affect aerial hyphal growth and surface hydrophobicity in *Ustilago maydis*. *EMBO J.* **15**, 4274–4281.
- Yang, Y.H., Dudoit, S., Luu, P., Lin, D.M., Peng, V., Ngai, J., and Speed, T.P.** (2002). Normalization for cDNA microarray data: A robust composite method addressing single and multiple slide systematic variation. *Nucleic Acids Res.* **30**, e15.
- Zuker, M.** (2003). Mfold web server for nucleic acid folding and hybridization prediction. *Nucleic Acids Res.* **31**, 3406–3415.

